

Preparation of high stable nanofluid based N-doped quantum dot in diethanolamine solution for carbon dioxide absorption



Peyman Moghaddam ^a, Mohammad Reza Ehsani ^a, Alimorad Rashidi ^{b,*}

^a Chemical Engineering Group, Pardis College, Isfahan University of Technology, Isfahan 8415683111, Iran

^b Nanotechnology Research Center, Research Institute of Petroleum Industry (RIPID), Tehran, Iran

ARTICLE INFO

Keywords:

CO₂ absorption

DEA

Chitosan

Carbon dot nanofluid

ABSTRACT

According to the increase of greenhouse gases such as CO₂ in the atmosphere following the growth and establishment of various industries, serious and rapid solutions for this challenge are required to prevent the release of this gas. CO₂ absorption in amine nanofluid is an emerging method nowadays. In this study, chitosan was synthesized from shrimp shells to prepare carbon dots (CDs). These CDs were treated by amino groups using the hydrothermal method. The structural properties of nanoparticles (NPs) were characterized by FT-IR, XRD, SEM, and zeta potential analyses and the NPs were quasi-spherical with regular micropores. The efficiency of CO₂ absorption from a gas mixture of CO₂/N₂ was considered as a percentage of the difference in CO₂ absorption capacities between nanofluid and diethanolamine (DEA, 10 wt%) solution compared to the CO₂ absorption capacity of DEA. The experimental results showed that the efficiency of CO₂ absorption for CDCH:N-200-8, CDCH:N-180-12, CDCH:N-200-12 and CDCH:N-180-8 nanofluids was equal to 73.86, 53.87, 49.25 and 22.88 %, respectively, which had increased CO₂ absorption significantly compared to the DEA base fluid. Among the synthesized samples, CDCH:N-200-8 nanofluid was a unique candidate for CO₂ capture from the atmosphere due to its high absorption efficiency since these particles had advantages such as ease of use, no corrosion, no deposition in the process, chemical inertness and high thermal stability.

1. Introduction

Increasing population and demand for energy have led to rising atmospheric temperature and global warming, which is one of the most fundamental problems in the world after the industrial revolution (Elhambakhsh et al., 2020; Lee et al., 2016). CO₂, as a greenhouse gas, is the most influential factor in global warming (Jiang et al., 2014). On the other hand, the enhancement of CO₂ concentration in the atmosphere causes some problems, such as severe tissue damage in the liver, pancreas, kidneys, and eyes and respiratory problems, threatening the health of humans and other living (Frommel et al., 2012). Also, the dissolution of this gas in rivers and seawater, leading to acidic water, is dangerous to the aqua system (Haigh et al., 2015; Rangwala, 1996). Additionally, industries have also intensified the CO₂ problems. In fact, CO₂ causes the production of bicarbonate ions and the subsequent corrosion phenomenon, decreasing the quality of industrial products (Groysman, 2017). Therefore, it is vital to remove CO₂ from the environment. There are various strategies for CO₂ capture, such as membrane technology, biologic, fuel cell, cryogenic, absorption and

adsorption (Campanari et al., 2013; Chen and Ahn, 2011; D'alessandro et al., 2010; Dashti et al., 2015; Mondal et al., 2012; Park et al., 2013; Sepehri and Sarrafzadeh, 2018; Spigarelli and Kawatra, 2013; Wong and Bioletti, 2002; Yu et al., 2012). Nevertheless, most of these methods are not suitable for CO₂ capture due to their high cost, brittleness, complex commercial-scale manufacture, complexity in manufacturing, too much-required energy for refrigeration, low CO₂ adsorption capacity, etc. (Elhambakhsh et al., 2020).

Due to the advantages of high CO₂ adsorption capacity and good adsorption kinetics, chemical adsorption technology by amine-based solutions has attracted much attention from researchers in CO₂ adsorption (Elhambakhsh et al., 2020). By adding carbon nanotube (CNT) to the base fluid, Ma et al. observed that the Brownian motion of the nanotubes led to local microconduction (Ma et al., 2007). They also stated that the grazing effect (absorption of the gas molecules by the nanosorbent surface and then their removal (Zhou et al., 2003)) by another mechanism increased the efficiency of NH₃ (Ma et al., 2007). Kang et al. investigated the absorption of CO₂ by carbon nanotubes. According to their observations, the mass transfer rate by nanofluid

* Corresponding author.

E-mail address: rashidiam@ripid.ir (A. Rashidi).

containing 0.001 wt% of CNT has increased compared to pure water by 20 % (Kang et al., 2007).

Pahlwanizadeh et al. investigated the mass transfer coefficient of CO₂ absorption by water/Fe₂O₃ nanofluid in a film-forming system in the regime of calm and turbulent streams. Their results indicated an improvement in the mass transfer coefficient in the presence of Fe₂O₃ nanoparticles in the turbulent stream compared to the regime with the calm stream. They found that at a constant Reynolds number and increasing the volume percentage of nanoparticles in the base fluid, the mass transfer coefficient was improved, and this amount was 13.7 % in the calm stream and 111 % in the turbulent stream at the nanoparticle concentration of 0.05 % v/v in the base fluid. They also found that the mass transfer coefficient in a magnetic field increased by 10 % and 29 % for water and nanofluid, respectively (Pahlevaninezhad et al., 2021).

One of the essential points in reactive adsorption is the selection of a suitable chemical solvent providing the desired needs, such as fast reaction kinetics, high energy savings for regeneration, high chemical and thermal stability and high adsorption capacity (Pashaei and Ghaemi, 2020; Pashaei et al., 2016). The most popular solvents used for industrial chemical absorbents include DEA (diethanolamine), MDEA (methyldiethanolamine), AMP (N-2-amino-2-methyl-1-propanol), MEA (monoethanolamine), DIPA (di isopropanolamine) and TEA (triethanolamine) (Du et al., 2017; Norouzbahari et al., 2016). Elhambakhsh et al. investigated CO₂ absorption using a nanofluid containing glutamine-linked Fe₂O₃ NPs in a high-pressure batch setup. They observed that at an optimal NP concentration of 0.05 wt% in water and pressure of 40 bar, the CO₂ absorption efficiency increased by approximately 33.93 % compared to the base fluid of water. Moreover, as pressure was changed from 20 to 40 bar, CO₂ absorption increased by about 1.5 times using Fe₂O₃@glutamine of 0.05 wt% (Elhambakhsh et al., 2021). Aref and Shahhosseini investigated the influence of the two-dimensional hexagonal boron nitride nanostructures (hBNs) upon CO₂ absorption into MDEA. The effect of hBNs loading and MDEA concentration on CO₂ absorption were evaluated. Results indicated that loading hBNs into MDEA up to a concentration of 0.025 wt% enhanced CO₂ absorption; further increasing the NP loading reduced the aforementioned value. Based on CO₂ absorption measurements, MDEA with 5 wt% containing 0.025 wt% of hBNs provided the highest enhancement of CO₂ absorption equals to 3.98 %. Furthermore, results revealed that higher MDEA concentrations weaken the enhancement effect of the nanofluids (Aref and Shahhosseini, 2023). Lashgarinejad et al. studied the ethylene diamine-functionalized Fe₃O₄@graphene oxide (NH₂-mGO) into MDEA for augmenting CO₂ absorption. They reported that novel nanofluid containing 0.1 wt% NH₂-mGO and 40 wt% MDEA improved the CO₂ absorption capacity by 19 % compared to the base fluid of 40 wt% MDEA (Lashgarinejad et al., 2023).

Zarei and Keshavarz perused the nanofluids of Fe₃O₄, CuO, ZnO and SiO₂ into the base fluid of MDEA for CO₂ absorption at ambient conditions in a bubble column reactor. Based on the CO₂ absorption results, Fe₃O₄ into MDEA with the NP concentration of 0.01 wt% had the highest CO₂ absorption capacity equals to 36 % improvement compared to MDEA; however, according to the stripping experiments at 70 °C, the CuO NPs at 0.05 wt% into MDEA had higher efficiency (Zarei and Keshavarz, 2023). Liang et al. appraised the nanofluid by adding TiO₂ as NPs and sodium polyacrylate as a surfactant into MDEA-MEA aqueous solution to improve CO₂ absorption performance. They apperceived that the aforementioned nanofluid with the composition of 0.6 g/L TiO₂, 25 % MDEA and 5 % MEA had a more significant enhancement in CO₂ absorption with enhancement factor up to 1.36 compared to single-component MEA/MDEA solution (Liang et al., 2022). Azizi et al. assessed the equilibrium absorption of CO₂ in an aqueous solution of DEA containing SiO₂ NPs. Results showed that the CO₂ solubility in the nanofluid increased with the raised pressure from 4 to 15 bar as well as the increased DAE concentration from 10 to 25 %. The optimal SiO₂ concentration was 0.5 wt%. In addition, more increases in NP concentration deteriorated the CO₂ solubility (Azizi et al., 2022). Among the

amines, DEAs have advantages such as high reactivity, suitable thermal stability and good economic efficiency, resulting in the superiority of this solvent over other solvents (Vaidya and Kenig, 2007). Oyevaar et al. used the reaction between CO₂ and aqueous DEA to determine the surface areas in a bubble column (Oyevaar et al., 1990). The study by Rinker et al. was about the absorption of CO₂ in an aqueous solution of DEA. They observed that increasing the gas flow velocity increased the removal of CO₂. Also, increasing the solution concentration, gas flow rate and decreasing partial pressure caused the mass transfer coefficient to increase (Rinker et al., 2000).

In the last two decades, nanotechnology and surface science advances have led to using nanofluids in the CO₂ absorption process. Nanofluids cannot solve problems (such as fouling, sedimentation, adhesion and corrosion) due to heterogeneous solid-liquid compounds containing micrometer or millimeter particles (Lee et al., 2010). Solvents such as nanofluids increase CO₂ absorption performance (Aghehrachaboki et al., 2019). The mechanism of mass transfer enhancement in nanofluids is not well known (Irani et al., 2018). In general, nanofluids have more thermal performance and mass transfer than basic amine fluids in gas absorption (Esmaili-Faraj and Nasr Esfahany, 2016).

The aquatic processing industry produces about 9.5 million tons of waste, of which about 1 ton is dedicated to the waste from shrimp and sea crustacean processing. In India as the third largest producer of fisheries in the world, shrimp production is estimated to be around 300,000 tons in 2013. Disposing of these waste materials is a major global problem faced by many seafood processing plants and has led to efforts to convert waste materials into value-added products such as chitosan. The application of chitosan could be increased by applying modifications to its amino and hydroxyl groups. The abundance of chitosan and the variety of modifications to its structure have led to its various biocompatible applications being effectively noticed by researchers (Bakshi et al., 2020).

Therefore, the synthesized chitosan from shrimp shells as a waste material impregnated on carbon dots (CDs) dispersed into the aqueous solution of DEA causes the CO₂ absorption capacity of DEA to improve by 73.86 %. The solution reduces the operating expenditures for a specific CO₂ absorption efficiency due to less consumption of DEA. In addition, using a mixture of chitosan & DEA instead of DEA solution alone causes less corrosion and more safety (i.e., health hazard and instability), decreasing the production cost. Using chitosan-derived adsorbents for CO₂ absorption has attracted the attention of researchers. Chemical inertness and thermal stability make these materials suitable for CO₂ absorption. The mechanism of CO₂ uptake by chitosan involves the formation of ammonium carbamate, which releases CO₂ gas upon heating (Pinto et al., 2011). Chitosan-based CO₂ adsorbents have an adsorption capacity of approximately four times that of crude chitosan (Chagas et al., 2020). As a result, in this study, chitosan-based CDs, which were synthesized from shrimp shells, were used for CO₂ absorption. CDs obtained from chitosan having nitrogen (amino groups). To improve the CO₂ absorption efficiency, CDs were functionalized with amino groups by hydrothermal method. It was observed that among the synthesized samples, CDCH:N-200-8 nanofluid had the highest absorption efficiency (73.86 %). Therefore, to our knowledge, this is the first study that has been performed. In summary, the article contributions are:

- Preparation of chitosan from shrimp shells to produce the CDs functionalized amino groups.
- Use the CDs-linked amino groups for the CO₂ capture from a gas mixture of CO₂/N₂ in a bubble column at continuous mode.
- Investigation of the thermal recovery of nanofluid toward CO₂ desorption.
- Study the mechanism of CO₂ absorption reaction into an amine nanofluid.

2. Experimental section

2.1. Materials

Sodium hydroxide (NaOH, pure), Hydrochloric acid (HCl 37 %, Merck), and Ammonium hydroxide solution (NH₄OH 25 %, Merck), Shrimp shell from the seafood market. All chemicals were used as received without further purification.

2.2. Synthesis of CH NPs

CH NPs were prepared using the following method (Gedda et al., 2016; Zahedi et al., 2018) (see Fig. 1). First, shrimp shell wastes were removed, washed with distilled water, dried at 60 °C for 12 h, and subsequently milled. Chitosan was synthesized in three subsequent steps:

- i) Deproteinization: 5 g of shrimp shell powders were mixed with 70 mL of NaOH (4 wt%) at 25 °C for 5 h. Then, powders were separated by filtration and washed with distilled water to reach pH = 7. Finally, the resulting powders are dried in an oven at 60 °C for 4 h to obtain chitin.
- ii) Demineralization: 1 g of chitin powder was mixed with 5 mL of HCl (3 wt%) at 90 °C for 1 h. The mixture was filtered and washed with distilled water to neutralize the pH, then dried in an oven at 60 °C for 4 h.
- iii) Deacetylation: At this stage, the obtained sample was refluxed with a more concentrated solution of NaOH (40–45 wt%) at a temperature of 80 °C for 2 h. The resulting solution was cooled to ambient temperature and then filtered. Finally, it was washed with distilled water and dried in an oven at 80 °C for 24 h.

2.3. Synthesis of CDs obtained from CH (CDCH:N)

CDCH:N was prepared by the hydrothermal method (Zattar et al., 2021). First, CH (1 g) was diluted in an acetic acid solution (50 mL, 2 wt %) and stirred for 48 h. 0.6 mL of NH₄OH solution (25 wt%) was added to the resulting mixture and sealed in an autoclave at 180 °C for 12 h. The autoclave was cooled to room temperature, and the mixture was centrifuged at a rate of 9000 RPM for 15 min. The resulting CDCH:Ns were filtered through 0.22 mm membranes and dried in a freezer for 48 h (see Fig. 1). The dried CDCH:Ns were coded as CDCH:N-180-12, CDCH:N-180-8, CDCH:N-200-12, and CDCH:N-200-8. The CDCH:N samples were also synthesized by the same method but with varying temperatures and times.

2.4. Experimental setup of CO₂ absorption

CO₂ uptake was investigated with CDs synthesized by a household bubble column under environmental conditions. As Fig. 2 shows, a mass rate controller (Alicat Model, MC Series, USA) was used to regulate the flow of incoming CO₂ gas (3000 ppm concentration) mixed with nitrogen gas.

A tube connects the gas capsule and the glass bubble column, which transfers the gas to the bubble column. The glass bubble is about 20 cm long, 4 cm in diameter and contains 100 mL of DEA/nanosolution. Also, a jacket is employed to adjust the room temperature of the solution. The gas flow rate was 150 mL/min and the CO₂ concentration in the cylinder was 3000 ppm (the capsule contains CO₂ and N₂). After CO₂ enters the bubble column, it is split into smaller bubbles by air stones to increase the contact surface. The column outlet bubbles contain an amount of moisture that must pass through a silica gel column (length of 15 cm and diameter of 5 cm) to remove the gas humidity and record the exact amount of CO₂ emitted by the CO₂ analyzer (Model Geotech, UK). Also, the setup includes a mass flow meter (Alicat model, MC series, USA) and a water circulation system to adjust the flow and temperature, respectively.

CO₂ absorption capacity is calculated from Eq. (1) (Haghtalab et al., 2015; Rahmatmand et al., 2016).

$$M = \left(\frac{QP}{RT} \right) \int_0^{\tau} \left(\frac{X_{in}}{Z_{in}} - \frac{X_{out}(t)}{Z_{out}} \right) dt \quad (1)$$

where the parameters of Q, T, P, X_{in}, X_{out}, Z_{in}, Z_{out}, R, t and τ indicate the flow rate, temperature, pressure, the molar fraction of CO₂ at the inlet, the molar fraction of CO₂ at the outlet, the factor of non-ideality gas at the inlet, the factor of non-ideality gas at the outlet, gas constant, time and end time, respectively.

Since the operating pressure is about 1 bar, the mixture of N₂ and CO₂ gas is assumed to be ideal. Thus, the non-ideal factors of inlet and outlet gas are considered 1. Also, the coefficient of CO₂ absorption by different nanofluids and DEA base fluid is calculated from Eq. (2) (Arshadi et al., 2019).

$$E = 100 \times \left(\frac{\int_0^{\tau} \left(\frac{X_{in}}{Z_{in}} - \frac{X_{out}(t)}{Z_{out}} \right) dt}{\int_0^{\tau} \left(\frac{X_{in}}{Z_{in}} - \frac{X_{out}(t)}{Z_{out}} \right) dt}_{\text{nanosolution}} - 1 \right) \frac{\int_0^{\tau} \left(\frac{X_{in}}{Z_{in}} - \frac{X_{out}(t)}{Z_{out}} \right) dt}{\int_0^{\tau} \left(\frac{X_{in}}{Z_{in}} - \frac{X_{out}(t)}{Z_{out}} \right) dt}_{\text{DEA solution}} \quad (2)$$

In addition, to ensure the absorption data, the absorption process of

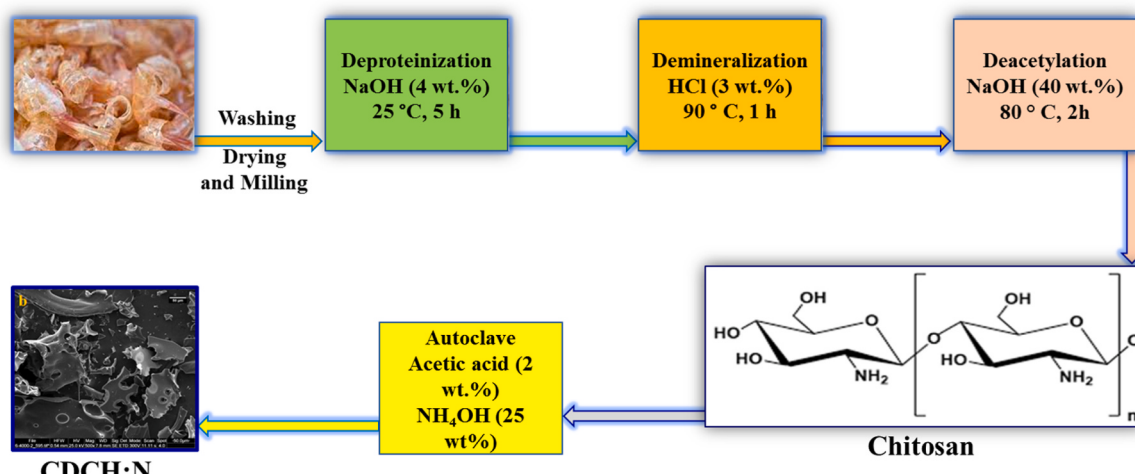


Fig. 1. CDCH:N synthesis steps from shrimp shell.

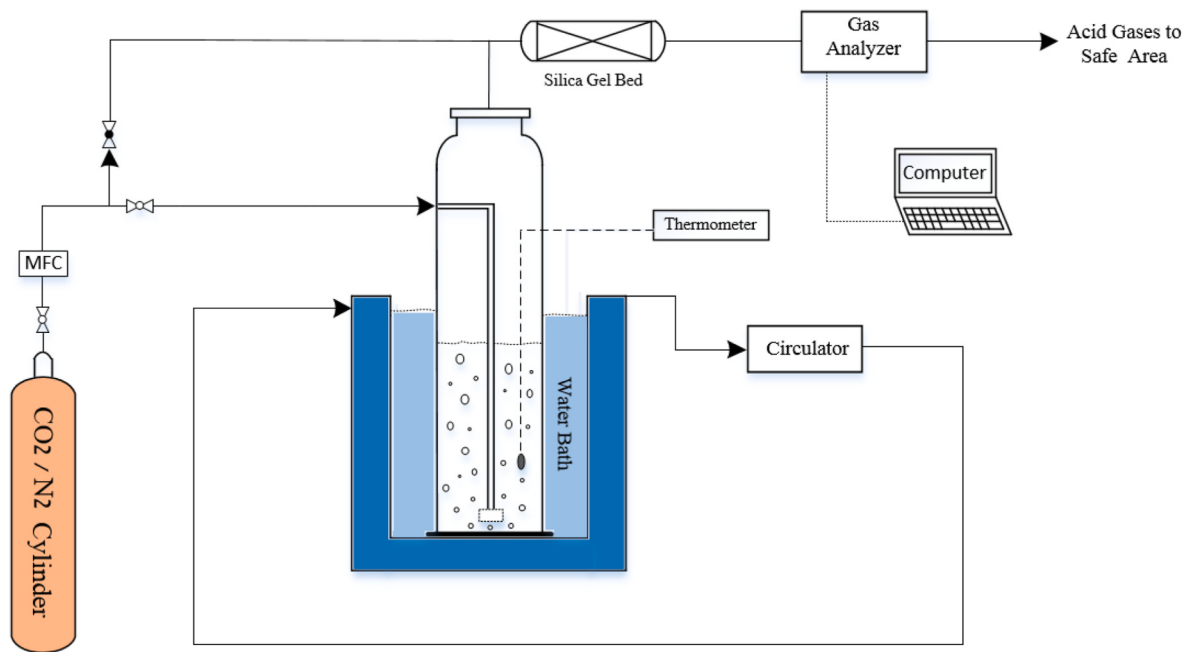


Fig. 2. Schematic image of a bubble column setup for CO_2 absorption.

CO_2 was repeated three times. Still, to reduce the irregularity in the graphs, only the graphs related to DEA and nanofluids have been reported (see Fig. 6).

Also, the CO_2 desorption from CDs in a bubble column at 40 °C and atmospheric pressure was performed. In this process, N_2 gas with a flow rate of 150 mL/min has been utilized according to the setup in Fig. 2 to purify the selected nanofluid solution CDCH: N-200-8 rich in CO_2 . The circulator device and oil bath (for uniform heat transfer) have been used to achieve the desired temperature of the desorption process. Moreover, a bubble tower is placed inside the oil bath. The ratio of the time to reach zero concentration of CO_2 gas at the outlet of the desorption tower for nanofluid compared to the base fluid is desired in this process.

3. Results and discussion

3.1. Characterization

Fig. 3 displays electron microscopy (SEM) images. According to these images, the CDs are quasi-spherical (Zhou et al., 2007). The smooth areas in the CDCH:N SEM indicate the regularity of the micropores. Also, the stability of the selected nanofluid (CDCH:N-200-8) was investigated using the zeta potential test, which shows that the sample has excellent stability (see Fig. 3c).

FT-IR analyses are used to investigate the functional groups on the surface of CDCH:Ns. The relevant results are reported in Fig. 4. The results confirmed the presence of NH groups in about 3200 cm^{-1} in all modified samples (Zattar et al., 2021). The peak in the wavenumber of 1665 cm^{-1} is associated with the C=O stretching of the amide of the CDCH:Ns (Zattar et al., 2021). Also, the peaks corresponding to the deformed and vibration NH groups and stretching CN appeared at 1570 cm^{-1} and 1280 cm^{-1} , respectively (Zattar et al., 2021). Considering the appearance of these peaks in the CDCH:Ns spectrum and comparing them with the FT-IR spectra of CH, it can be concluded that the synthesis of the samples was successful.

The X-ray diffraction pattern (XRD) was used to study the crystallinity of the CDs (see Fig. 5). The XRD spectrum shows a broad peak at $2\theta = 22.48^\circ$, similar to the graphite lattice distance. This peak is related to amorphous carbon atoms (Liu et al., 2016; Wang et al., 2010, 2014).

3.2. Study of CO_2 absorption and desorption of CDCH:Ns

In this research work, DEA was used as a base fluid to investigate the efficiency of synthesized CDs nanofluid in CO_2 uptake. Because, they have high reactivity, good thermal stability and suitable economic efficiency. The results of CO_2 absorption versus time for DEA aqueous solution and CDCH:N-180-12, CDCH:N-200-12, CDCH:N-200-8 and CDCH:N-180-8 nanofluids at concentrations of 0.005–0.1 wt% are shown in Fig. 6a–d. The CO_2 absorption capacity of the base fluid of 10 wt% DEA was 0.124 mmol CO_2 /mL. The results revealed that adding NPs has increased the absorption of CO_2 compared to the base fluid, which confirms the presence of amino groups, significantly increasing the solubility of NPs in the base solvent. The results of SEM analyses and XRD spectra indicate favorable conditions such as the quasi-spherical shape of nanoparticles, the regularity of micropores and the appropriate lattice structure to improve CO_2 absorption (Elhambakhsh et al., 2020). Based on the FT-IR analyses, the functionalization of CDs with the amino groups supplied by chitosan has increased CO_2 absorption compared to the base fluid of DEA, which is in line with the results of other researchers (Aref and Shahhosseini, 2023; Azizi et al., 2022; Elhambakhsh et al., 2020, 2021). At low concentrations of NPs, the low viscosity causes the reactive sites of CDCH: N samples to change, so the dispersion of the adsorbent in the aqueous solution is easily accomplished, during which the mass transfer reduces (Lee et al., 2015).

CDCH: Nanofluid N-200-8 (0.05 wt%) shows the highest density of active sites and more favorable chemical interaction with CO_2 , which is demonstrated through its high gas absorption (73.86 %) (see Fig. 6c). After the NPs concentration reaches 0.5 wt%, the layer thickness adjacent to the bubble and the liquid interface in the nanofluid decrease because the bubble boundary layer is surrounded more rapidly by the NPs. As a result, mass transfer into the liquid film increases (Kim et al., 2014).

On the other hand, increasing the NPs to 0.1 wt% reduces the Brownian motion and attraction between particles due to enhanced collision and accumulation of these NPs. Therefore, the active sites block, the total surface area decreases and CO_2 absorption diffusion path length increases. So, it can be concluded that mass diffusion decreases (Krishnamurthy et al., 2006; Lee et al., 2011). According to these results, a 0.05 wt% sample was selected as the optimal value due to no

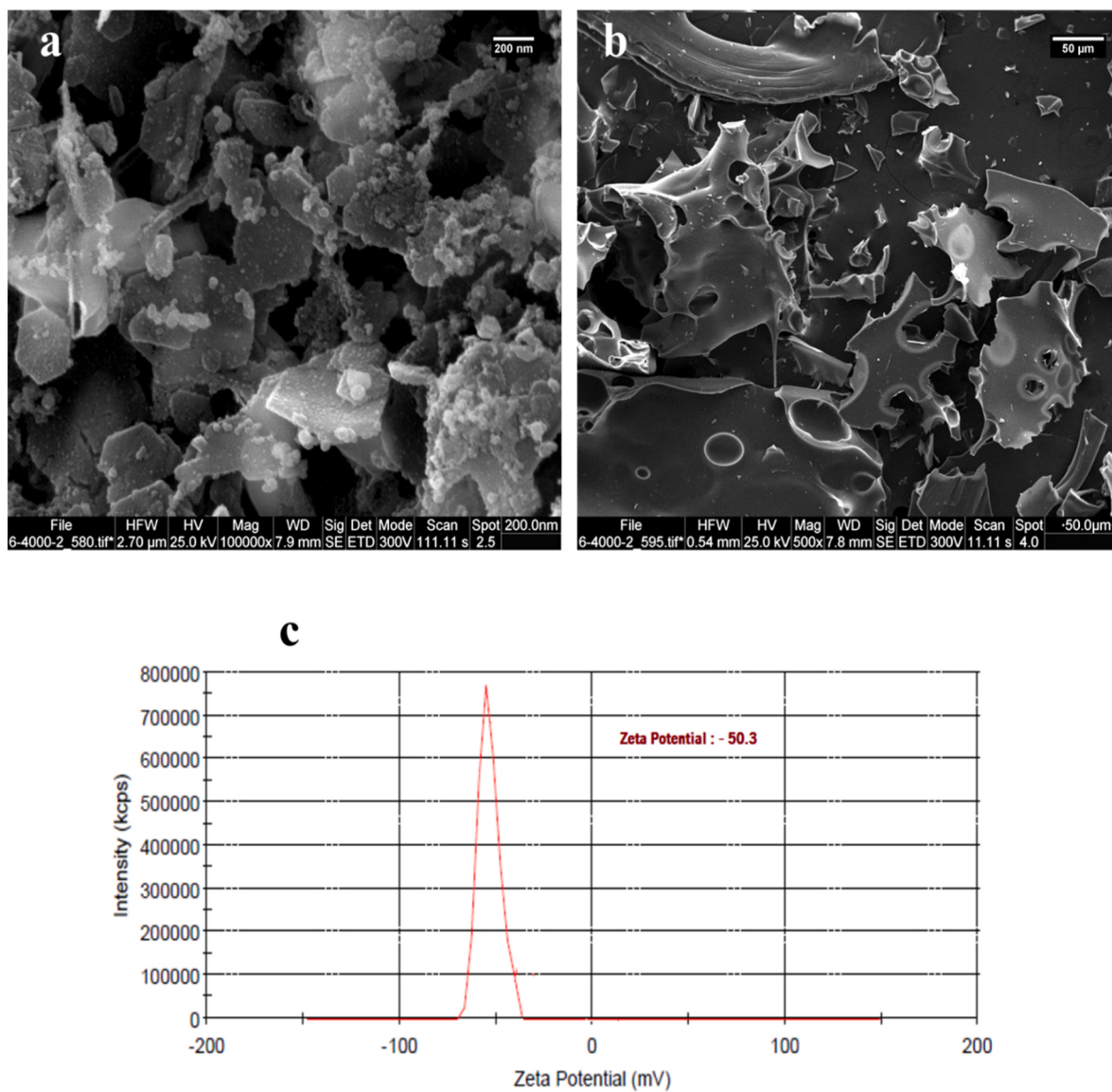


Fig. 3. SEM images of a) CH and b) CDCH:N-200-8; c) zeta potential result of CDCH:N-200-8.

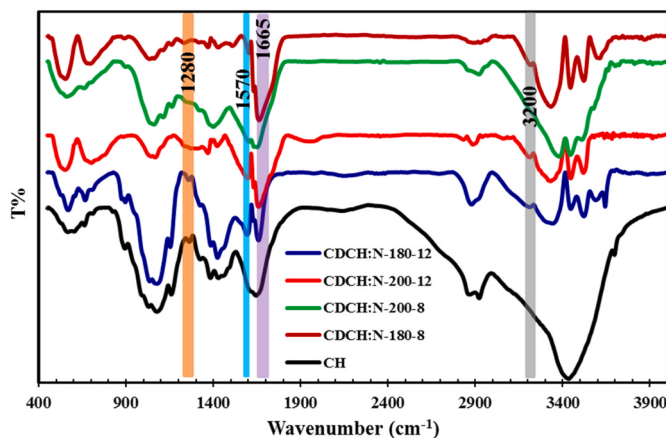


Fig. 4. FT-IR spectra of CH and CDCH:Ns.

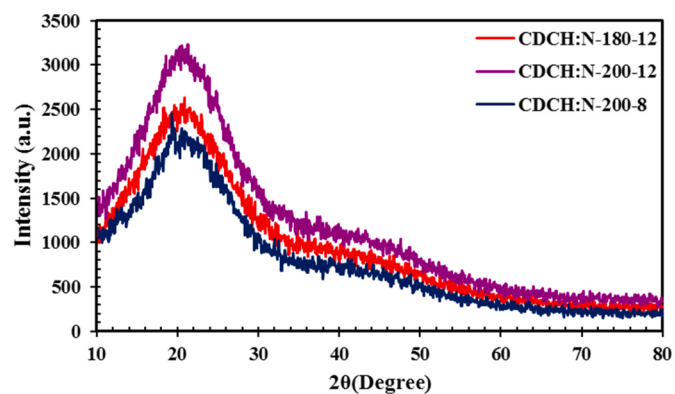


Fig. 5. XRD pattern of CDCH:Ns sample.

aggregation according to the zeta potential value of -50 mV (Ali et al., 2018) and the high density of active sites (Elhambahksh et al., 2020).

On the other hand, according to the desorption graphs in Fig. 7, it was observed that the CO_2 desorption rate for all CD samples decreased

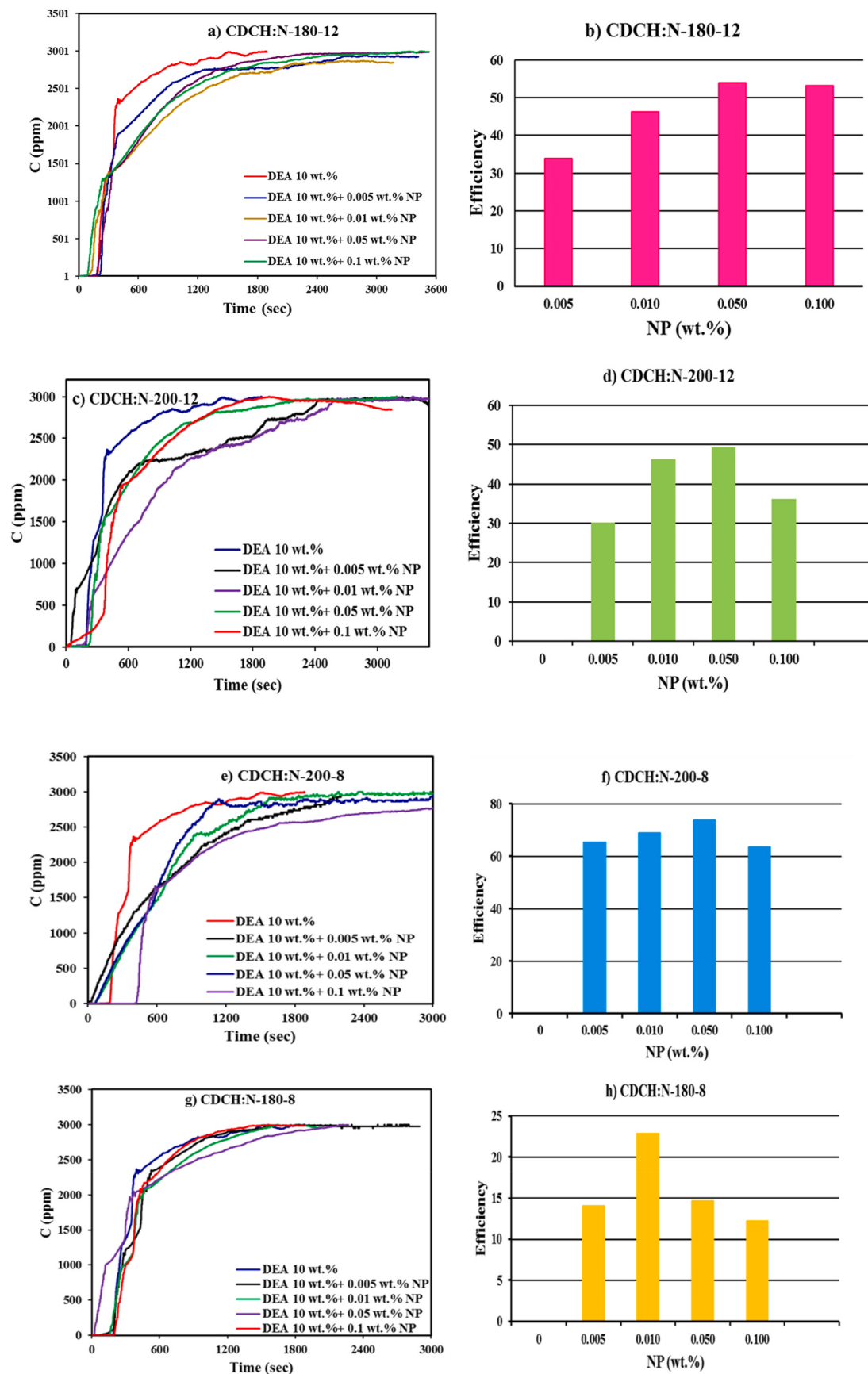


Fig. 6. a, c, e and g) CO₂ absorption curves of nanofluids at various concentrations; b, d, f and h) Effect of CDCH:Ns loading on CO₂ absorption.

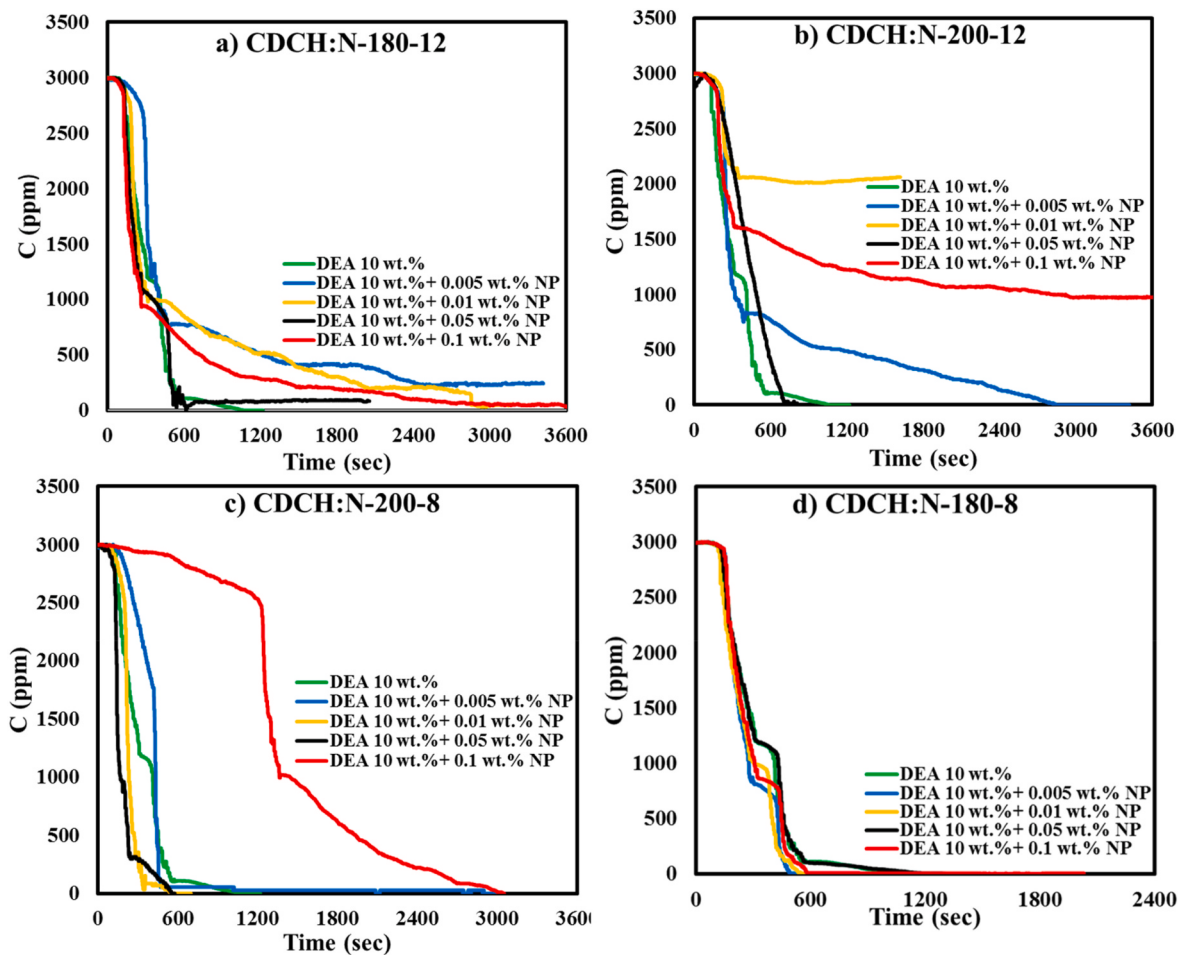


Fig. 7. CO_2 desorption curves of nanofluids at various concentrations.

rapidly with an increasing amount of NPs, and then gradually decreased to zero. Samples CDCH:N-180-12, CDCH:N-200-12 and CDCH:N-180-8 have a higher function group. Since the desorption took place under low temperature (40°C), it prevents the release of gas, but the better desorption of sample CDCH:N-200-8 is observed due to its high porosity, which causes the release of CO_2 gas.

3.3. Mechanism of CO_2 absorption reaction

The interaction between CO_2 and amino groups of nanosorbents is a function of anionic and cationic mechanisms (see Fig. 8). When CO_2 (anionic component) is exposed to amino groups (cationic component) of nanofluid, it produces intermediate carbamate groups, protonating the NPs surface and finally stabilizing the CO_2 on the nanosorbent surface (Eq.s (3)–(6)) (Boot-Handford et al., 2014; Robinson et al., 2012).



In other words, the investigation of the results shows that with the increased concentration of NPs, the absorption of CO_2 improves and decreases significantly. Increasing the NPs concentration to 0.05 wt% around the gas bubbles causes the gas bubbles to break into smaller bubbles, increases the liquid-gas contact, reduces the thickness of the diffusion boundary layer and, as a result, the mass transfer improves. In

other words, the hydrodynamic effect of NPs leads to improve diffusion and mass transfer in the liquid film around the gas bubbles. On the other hand, increasing the concentration to more than 0.05 wt% causes the aggregation of NPs and increases their collision with one another. Therefore, the Brownian motion of NPs and, finally, the effect of active sites of NPs decreased. In general, at concentrations higher than the optimal value, the inhibition of the interaction between CO_2 and active sites increases and as a result, the absorption of CO_2 decreases.

3.4. Comparison of CO_2 absorption efficiency by CDCH:N described in this work with other nanosorbents

One of the critical factors of adsorbents is their absorption efficiency. Table 1 compares the nanosorbent used in this work with the other reported nanosorbents. The results show that this nanosorbent has excellent absorption efficiency toward CO_2 .

4. Conclusions

In this work, the amount of CO_2 absorption/desorption and CO_2 absorption efficiency into DEA nanofluid in the presence of four nanosorbents, including CDCH:N-200-8, CDCH:N-180-12, CDCH:N-200-12 and CDCH:N-180-8 were studied using a bubble column under ambient conditions and continuous mode. The conclusions are as follows:

- CDs were prepared using chitosan synthesized from shrimp shells by the hydrothermal method and finally treated with amino groups to

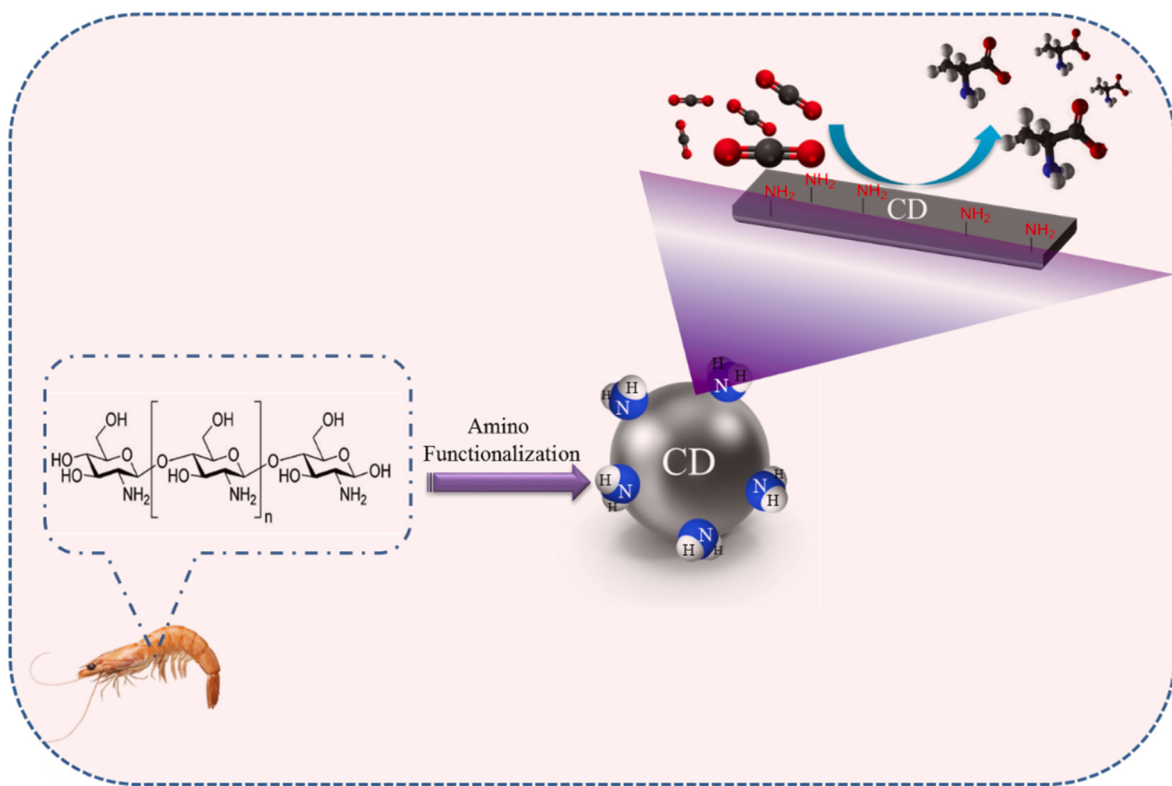


Fig. 8. Mechanism of CO₂ absorption reaction.

Table 1
Comparison of CDCH: N-200-8 absorption efficiency with other nanosorbents.

Nanosorbents	Absorbent loading	Absorption capacity (%)	Solvent type	Contactor type	Ref.
CDCH:N-200-8	0.05 wt%	73.86	DEA	Bubble column	This work
SiO ₂	0.021 wt%	24	Water	Wetted wall column	Wang et al. (2015)
r-Al ₂ O ₃	1 vol%	40–55	Water	Wetted wall column	Samadi et al. (2014)
α-Al ₂ O ₃	0.01 vol%	4.5	Methanol	Bubble absorber	Lee et al. (2011)
α-Al ₂ O ₃	0.05 vol%	9.4	Methanol	Tray column absorber	Pineda et al. (2012)
Fe ₃ O ₄	0.025 wt%	18.1	Water	Bubble column absorber	Elhambakhsh et al. (2020)
Fe ₂ O ₃	0.025 wt%	16	Water	Batch vessel	Elhambakhsh et al. (2021)
CNT	0.02 wt%	23	MDEA	Batch vessel	Rahmatmand et al. (2016)
SiO ₂	0.1 wt%	21	Water	Batch vessel	Rahmatmand et al. (2016)
Fe ₃ O ₄	0.02 wt%	24	Water	Batch vessel	Rahmatmand et al. (2016)
CNT	0.02 wt%	34	Water	Batch vessel	Rahmatmand et al. (2016)
SiO ₂	0.021 wt%	24	Water	Bubble column	Kim et al. (2008)
CNT	0.2 wt%	20	14.08 wt% NH ₃ /water	Bubble column	Ma et al. (2009)

increase the CO₂ absorption efficiency from the gas mixture of CO₂/N₂ with the CO₂ concentration of 3000 ppm and gas flow rate of 150 mL/min.

- Based on the SEM images, the CDs were quasi-spherical with the regularity of the micropores. Moreover, the FT-IR analyses confirmed the successful functionalization of amino groups on the surface of CDCH:Ns.
- The efficiency of CO₂ absorption for CDCH:N-200-8, CDCH:N-180-12, CDCH:N-200-12 and CDCH:N-180-8 nanofluids were equal to 73.86, 53.87, 49.25 and 22.88 %, respectively, which has increased CO₂ absorption significantly compared to DEA base fluid.
- CDCH:N-200-8 sample with an optimal concentration of 0.05 wt% into DEA of 10 wt% showed better CO₂ absorption efficiency due to its high porosity. Furthermore, the prominent factors influencing CO₂ absorption using a nanofluid are the hydrodynamic contact effect and Brownian motion.

- Results of the nanofluid thermal recovery showed that the CO₂ desorption rate for all CD samples decreased rapidly with an increasing amount of NPs and then gradually reached zero.

Funding

Not applicable.

Availability of data and materials

The data sets used and/or analyzed during the current study are available from the corresponding author upon reasonable request.

CRediT authorship contribution statement

Peyman Moghaddam: Conceptualization, Methodology, Formal analysis, Software, Validation, Investigation, Writing – original draft, Visualization. **Mohammad Reza Ehsani:** Conceptualization,

Methodology, Resources, Writing – review & editing, Supervision, Project administration. **Alimorad Rashidi:** Conceptualization, Methodology, Resources, Writing – review & editing, Supervision, Project administration.

Declaration of competing interest

The authors declare that they have no known competing financial interests or personal relationships that could have appeared to influence the work reported in this paper.

Data availability

No data was used for the research described in the article.

Acknowledgment

The authors are grateful to the Isfahan University of Technology and the Research Institute of Petroleum Industry for supporting this research.

References

- Aghehrochaboki, R., Chaboki, Y.A., Maleknia, S.A., Irani, V., 2019. Polyethyleneimine functionalized graphene oxide/methyl diethanolamine nanofluid: Preparation, characterization, and investigation of CO₂ absorption. *J. Environ. Chem. Eng.* 7 (5), 103285. <https://doi.org/10.1016/j.jece.2019.103285>.
- Ali, N., Teixeira, J.A., Addali, A., 2018. A review on nanofluids: fabrication, stability, and thermophysical properties. *J. Nanomater.* 2018. <https://doi.org/10.1155/2018/6978130>.
- Aref, A.H., Shahhosseini, S., 2023. Experimental investigation of carbon dioxide absorption by amine-based nanofluids containing two-dimensional hexagonal boron nitride nanostructures. *Gas Sci. Eng.* 111, 204917. <https://doi.org/10.1016/j.gscs.2023.204917>.
- Arshadi, M., Taghvaei, H., Abdolmaleki, M.K., Lee, M., Eskandarloo, H., Abbaspourrad, A., 2019. Carbon dioxide absorption in water/nanofluid by a symmetric amine-based dendritic adsorbent. *Appl. Energy* 242, 1562–1572. <https://doi.org/10.1016/j.apenergy.2019.03.105>.
- Azizi, S., Peyghambarzadeh, S.M., Yousefi, M., Abedpour, R., 2022. Experimental and statistical analysis of CO₂ absorption in DEA/water nanofluid containing silicon dioxide nanoparticle. *Part. Sci. Technol.* 1–9. <https://doi.org/10.1080/02726351.2022.2134065>.
- Bakshi, P.S., Selvakumar, D., Kadirvelu, K., Kumar, N.S., 2020. Chitosan as an environment friendly biomaterial—a review on recent modifications and applications. *Int. J. Biol. Macromol.* 150, 1072–1083. <https://doi.org/10.1016/j.ijbiomac.2019.10.113>.
- Boot-Handford, M.E., Abanades, J.C., Anthony, E.J., Blunt, M.J., Brandani, S., Mac Dowell, N., Fernández, J.R., Ferrari, M.C., Gross, R., Hallett, J.P., 2014. Carbon capture and storage update. *Energy Environ. Sci.* 7 (1), 130–189. <https://doi.org/10.1039/C3EE42350F>.
- Campanari, S., Manzolini, G., Chiesa, P., 2013. Using MCFC for high efficiency CO₂ capture from natural gas combined cycles: comparison of internal and external reforming. *Appl. Energy* 112, 772–783. <https://doi.org/10.1016/j.apenergy.2013.01.045>.
- Chagas, J.A.O., Crispim, G.O., Pinto, B.P., San Gil, R.A.S., Mota, C.J.A., 2020. Synthesis, characterization, and CO₂ uptake of adsorbents prepared by hydrothermal carbonization of chitosan. *ACS Omega* 5 (45), 29520–29529. <https://doi.org/10.1021/acsomega.0c04470>.
- Chen, C., Ahn, W.S., 2011. CO₂ capture using mesoporous alumina prepared by a sol-gel process. *Chem. Eng. J.* 166 (2), 646–651. <https://doi.org/10.1016/j.cej.2010.11.038>.
- D'alessandro, D.M., Smit, B., Long, J.R., 2010. Carbon dioxide capture: prospects for new materials. *Angew. Chem. Int. Ed.* 49 (35), 6058–6082. <https://doi.org/10.1002/anie.201000431>.
- Dashti, H., Yew, L.Z., Lou, X., 2015. Recent advances in gas hydrate-based CO₂ capture. *J. Nat. Gas Sci. Eng.* 23, 195–207. <https://doi.org/10.1016/j.jngse.2015.01.033>.
- Du, Y., Wang, Y., Rochelle, G.T., 2017. Piperazine/4-hydroxy-1-methylpiperidine for CO₂ capture. *Chem. Eng. J.* 307, 258–263. <https://doi.org/10.1016/j.cej.2016.08.095>.
- Elhambaksh, A., Ghanaatian, A., Keshavarz, P., 2021. "Glutamine functionalized iron oxide nanoparticles for high-performance carbon dioxide absorption". *J. Nat. Gas Sci. Eng.* 94, 104081. <https://doi.org/10.1016/j.jngse.2021.104081>.
- Elhambaksh, A., Zaeri, M.R., Mehdipour, M., Keshavarz, P., 2020. Synthesis of different modified magnetic nanoparticles for selective physical/chemical absorption of CO₂ in a bubble column reactor. *J. Environ. Chem. Eng.* 8 (5), 104195. <https://doi.org/10.1016/j.jece.2020.104195>.
- Esmaili-Faraj, S.H., Nasr Esfahany, M., 2016. Absorption of hydrogen sulfide and carbon dioxide in water based nanofluids. *Ind. Eng. Chem. Res.* 55 (16), 4682–4690. <https://doi.org/10.1021/acs.iecr.5b04816>.
- Frommel, A.Y., Maneja, R., Lowe, D., Malzahn, A.M., Geffen, A.J., Folkvord, A., Piatkowski, U., Reusch, T.B.H., Clemmesen, C., 2012. Severe tissue damage in Atlantic cod larvae under increasing ocean acidification. *Nat. Clim. Change* 2 (1), 42–46. <https://doi.org/10.1038/nclimate1324>.
- Gedda, G., Lee, C.Y., Lin, Y.C., Wu, H.F., 2016. Green synthesis of carbon dots from prawn shells for highly selective and sensitive detection of copper ions. *Sensor. Actuator. B Chem.* 224, 396–403. <https://doi.org/10.1016/j.snb.2015.09.065>.
- Groysman, A., 2017. Corrosion problems and solutions in oil, gas, refining and petrochemical industry. *Koroze a ochrana materialu* 61 (3), 100–117. <https://doi.org/10.1515/kom-2017-0013>.
- Haghtalab, A., Mohammadi, M., Fakhroueian, Z., 2015. Absorption and solubility measurement of CO₂ in water-based ZnO and SiO₂ nanofluids. *Fluid Phase Equil.* 392, 33–42. <https://doi.org/10.1016/j.fluid.2015.02.012>.
- Haigh, R., Ianson, D., Holt, C.A., Neate, H.E., Edwards, A.M., 2015. Effects of ocean acidification on temperate coastal marine ecosystems and fisheries in the Northeast Pacific. *PLoS One* 10 (2), e0117533. <https://doi.org/10.1371/journal.pone.0117533>.
- Irani, V., Tavasoli, A., Vahidi, M., 2018. Preparation of amine functionalized reduced graphene oxide/methyl diethanolamine nanofluid and its application for improving the CO₂ and H₂S absorption. *J. Colloid Interface Sci.* 527, 57–67. <https://doi.org/10.1016/j.jcis.2018.05.018>.
- Jiang, J., Zhao, B., Zhuo, Y., Wang, S., 2014. Experimental study of CO₂ absorption in aqueous MEA and MDEA solutions enhanced by nanoparticles. *Int. J. Greenh. Gas Control* 29, 135–141. <https://doi.org/10.1016/j.ijggc.2014.08.004>.
- Kang, Y.T., Lee, J.K., Kim, B.C., Year, 2007. *Absorption Heat Transfer Enhancement in Binary Nanofluids*. Int. Congr. Refrigeration. Beijing. ICR07-B2-371.
- Kim, J.H., Jung, C.W., Kang, Y.T., 2014. Mass transfer enhancement during CO₂ absorption process in methanol/Al₂O₃ nanofluids. *Int. J. Heat Mass Tran.* 76, 484–491. <https://doi.org/10.1016/j.ijheatmasstransfer.2014.04.057>.
- Kim, W.G., Kang, H.U., Jung, K.M., Kim, S.H., 2008. Synthesis of silica nanofluid and application to CO₂ absorption. *Separ. Sci. Technol.* 43 (11–12), 3036–3055. <https://doi.org/10.1080/01496390802063804>.
- Krishnamurthy, S., Bhattacharya, P., Phelan, P.E., Prasher, R.S., 2006. Enhanced mass transport in nanofluids. *Nano Lett.* 6 (3), 419–423. <https://doi.org/10.1021/nl0522532>.
- Lashgarinejad, A., Hosseini, S.S., Irani, V., Ghasemi, M.H., Mohammadpour, R., Tavasoli, A., 2023. Enhancement of CO₂ absorption and heat transfer properties using amine functionalized magnetic graphene oxide/MDEA nanofluid. *J. Iran. Chem. Soc.* 1–14. <https://doi.org/10.1007/s13738-023-02783-0>.
- Lee, J.K., Koo, J., Hong, H., Kang, Y.T., 2010. The effects of nanoparticles on absorption heat and mass transfer performance in NH₃/H₂O binary nanofluids. *Int. J. Refrig.* 33 (2), 269–275. <https://doi.org/10.1016/j.ijrefrig.2009.10.004>.
- Lee, J.S., Lee, J.W., Kang, Y.T., 2015. CO₂ absorption/regeneration enhancement in DI water with suspended nanoparticles for energy conversion application. *Appl. Energy* 143, 119–129. <https://doi.org/10.1016/j.apenergy.2015.01.020>.
- Lee, J.W., Jung, J.Y., Lee, S.G., Kang, Y.T., 2011. CO₂ bubble absorption enhancement in methanol-based nanofluids. *Int. J. Refrig.* 34 (8), 1727–1733. <https://doi.org/10.1016/j.ijrefrig.2011.08.002>.
- Lee, J.W., Pineda, I.T., Lee, J.H., Kang, Y.T., 2016. Combined CO₂ absorption/regeneration performance enhancement by using nanoabsorbents. *Appl. Energy* 178, 164–176. <https://doi.org/10.1016/j.apenergy.2016.06.048>.
- Liang, J., Han, H., Li, W., Ma, X., Xu, L., 2022. Experimental study on the absorption enhancement of CO₂ by MDEA-MEA based nanofluids. *Can. J. Chem. Eng.* 100 (11), 3335–3344. <https://doi.org/10.1002/cjce.24322>.
- Liu, X., Pang, J., Xu, F., Zhang, X., 2016. Simple approach to synthesize amino-functionalized carbon dots by carbonization of chitosan. *Sci. Rep.* 6 (1), 1–8. <https://doi.org/10.1038/srep31100>.
- Ma, X., Su, F., Chen, J., Bai, T., Han, Z., 2009. Enhancement of bubble absorption process using a CNTs-ammonia binary nanofluid. *Int. Commun. Heat Mass Tran.* 36 (7), 657–660. <https://doi.org/10.1016/j.icheatmasstransfer.2009.02.016>.
- Ma, X., Su, F., Chen, J., Zhang, Y., 2007. Heat and mass transfer enhancement of the bubble absorption for a binary nanofluid. *J. Mech. Sci. Technol.* 21 (11), 1813. <https://doi.org/10.1007/BF03177437>.
- Mondal, M.K., Balsora, H.K., Varshney, P., 2012. Progress and trends in CO₂ capture/separation technologies: a review. *Energy* 46 (1), 431–441. <https://doi.org/10.1016/j.energy.2012.08.006>.
- Norouzbahari, S., Shahhosseini, S., Ghaemi, A., 2016. Chemical absorption of CO₂ into an aqueous piperazine (PZ) solution: development and validation of a rigorous dynamic rate-based model. *RSC Adv.* 6 (46), 40017–40032. <https://doi.org/10.1039/C5RA27869D>.
- Oyevar, M.H., Morssinkhof, R.W.J., Westerterp, K.R., 1990. The kinetics of the reaction between CO₂ and diethanolamine in aqueous ethyleneglycol at 298 K: a viscous gas–liquid reaction system for the determination of interfacial areas in gas–liquid contactors. *Chem. Eng. Sci.* 45 (11), 3283–3298. [https://doi.org/10.1016/0009-2509\(90\)80220-9](https://doi.org/10.1016/0009-2509(90)80220-9).
- Pahlevaninezhad, M., Etesami, N., Nasr Esfahany, M., 2021. Improvement of CO₂ absorption by Fe3O4/water nanofluid falling liquid film in presence of the magnetic field. *Can. J. Chem. Eng.* 99 (2), 519–529. <https://doi.org/10.1002/cjce.23883>.
- Park, S., Lee, S., Lee, Y., Lee, Y., Seo, Y., 2013. Hydrate-based pre-combustion capture of carbon dioxide in the presence of a thermodynamic promoter and porous silica gels. *Int. J. Greenh. Gas Control* 14, 193–199. <https://doi.org/10.1016/j.ijggc.2013.01.026>.
- Pashaei, H., Ghaemi, A., 2020. CO₂ absorption into aqueous diethanolamine solution with nano heavy metal oxide particles using stirrer bubble column: hydrodynamics and mass transfer. *J. Environ. Chem. Eng.* 8 (5), 104110. <https://doi.org/10.1016/j.jece.2020.104110>.

- Pashaei, H., Ghaemi, A., Nasiri, M., 2016. Modeling and experimental study on the solubility and mass transfer of CO₂ into aqueous DEA solution using a stirrer bubble column. *RSC Adv.* 6 (109), 108075–108092. <https://doi.org/10.1039/C6RA22589F>.
- Pineda, I.T., Lee, J.W., Jung, I., Kang, Y.T., 2012. CO₂ absorption enhancement by methanol-based Al₂O₃ and SiO₂ nanofluids in a tray column absorber. *Int. J. Refrig.* 35 (5), 1402–1409. <https://doi.org/10.1016/j.ijrefrig.2012.03.017>.
- Pinto, M.L., Mafra, L., Guil, J.M., Pires, J., Rocha, J., 2011. Adsorption and activation of CO₂ by amine-modified nanoporous materials studied by solid-state NMR and ¹³CO₂ adsorption. *Chem. Mater.* 23 (6), 1387–1395. <https://doi.org/10.1021/cm1029563>.
- Rahmatmand, B., Keshavarz, P., Ayatollahi, S., 2016. Study of absorption enhancement of CO₂ by SiO₂, Al₂O₃, CNT, and Fe₃O₄ nanoparticles in water and amine solutions. *J. Chem. Eng. Data* 61 (4), 1378–1387. <https://doi.org/10.1021/acs.jcd.5b00442>.
- Rangwala, H.A., 1996. Absorption of carbon dioxide into aqueous solutions using hollow fiber membrane contactors. *J. Membr. Sci.* 112 (2), 229–240. [https://doi.org/10.1016/0376-7388\(95\)00293-6](https://doi.org/10.1016/0376-7388(95)00293-6).
- Rinker, E.B., Ashour, S.S., Sandall, O.C., 2000. Absorption of carbon dioxide into aqueous blends of diethanolamine and methylidethanolamine. *Ind. Eng. Chem. Res.* 39 (11), 4346–4356. <https://doi.org/10.1021/ie990850r>.
- Robinson, K., Mccluskey, A., Attalla, M.I., 2012. An ATR-FTIR study on the effect of molecular structural variations on the CO₂ absorption characteristics of heterocyclic amines, Part II. *ChemPhysChem* 13 (9), 2331–2341. <https://doi.org/10.1002/cphc.201200066>.
- Samadi, Z., Haghshenasfard, M., Moheb, A., 2014. CO₂ absorption using nanofluids in a wetted-wall column with external magnetic field. *Chem. Eng. Technol.* 37 (3), 462–470. <https://doi.org/10.1002/ceat.201300339>.
- Sepehri, A., Sarrafzadeh, M.H., 2018. Effect of nitrifiers community on fouling mitigation and nitrification efficiency in a membrane bioreactor. *Chem. Eng. Process. Process Intensification* 128, 10–18. <https://doi.org/10.1016/j.cep.2018.04.006>.
- Spigarelli, B.P., Kawatra, S.K., 2013. Opportunities and challenges in carbon dioxide capture. *J. CO₂ Util.* 1, 69–87. <https://doi.org/10.1016/j.jcou.2013.03.002>.
- Vaidya, P.D., Kenig, E.Y., 2007. CO₂-alkanolamine reaction kinetics: a review of recent studies. *Chem. Eng. Technol.: Ind. Chem. Plant Equip. Process Eng. Biotechnol.* 30 (11), 1467–1474. <https://doi.org/10.1002/ceat.200700268>.
- Wang, F., Kreiter, M., He, B., Pang, S., Liu, C.Y., 2010. Synthesis of direct white-light emitting carbogenic quantum dots. *Chem. Commun.* 46 (19), 3309–3311. <https://doi.org/10.1039/C002206C>.
- Wang, T., Yu, W., Fang, M., He, H., Xiang, Q., Ma, Q., Xia, M., Luo, Z., Cen, K., 2015. Wetted-wall column study on CO₂ absorption kinetics enhancement by additive of nanoparticles. *Greenhouse Gases: Sci. Technol.* 5 (5), 682–694. <https://doi.org/10.1002/ghg.1509>.
- Wang, W., Li, Y., Cheng, L., Cao, Z., Liu, W., 2014. Water-soluble and phosphorus-containing carbon dots with strong green fluorescence for cell labeling. *J. Mater. Chem. B* 2 (1), 46–48. <https://doi.org/10.1039/C3TB21370F>.
- Wong, S., Bioletti, R., 2002. Carbon Dioxide Separation Technologies. Alberta Research Council.
- Yu, C.H., Huang, C.H., Tan, C.S., 2012. A review of CO₂ capture by absorption and adsorption. *Aerosol Air Qual. Res.* 12 (5), 745–769. <https://doi.org/10.4209/aaqr.2012.05.0132>.
- Zahedi, S., Ghomi, J.S., Shahbazi-Alavi, H., 2018. Preparation of chitosan nanoparticles from shrimp shells and investigation of its catalytic effect in diastereoselective synthesis of dihydropyrroles. *Ultrason. Sonochem.* 40, 260–264. <https://doi.org/10.1016/j.ultsonch.2017.07.023>.
- Zarei, F., Keshavarz, P., 2023. Intensification of CO₂ absorption and desorption by metal/non-metal oxide nanoparticles in bubble columns. *Environ. Sci. Pollut. Control Ser.* 30 (7), 19278–19291. <https://doi.org/10.1007/s11356-022-23577-6>.
- Zattar, A.P.P., Fajardo, G.L., De Mesquita, J.P., Pereira, F.V., 2021. Luminescent carbon dots obtained from chitosan: a comparison between different methods to enhance the quantum yield. *Fullerenes, Nanotub. Carbon Nanostruct.* 29 (6), 414–422. <https://doi.org/10.1080/1536383X.2020.1854742>.
- Zhou, J., Booker, C., Li, R., Zhou, X., Sham, T.K., Sun, X., Ding, Z., 2007. An electrochemical avenue to blue luminescent nanocrystals from multiwalled carbon nanotubes (MWCNTs). *J. Am. Chem. Soc.* 129 (4), 744–745. <https://doi.org/10.1021/ja0669070>.
- Zhou, M., Cai, W.F., Xu, C.J., 2003. A new way of enhancing transport process –The hybrid process accompanied by ultrafine particles. *Kor. J. Chem. Eng.* 20 (2), 347–353. <https://doi.org/10.1007/BF02697251>.